Pressure-driven water infiltration into carbon nanotube: The effect of applied charges

Ling Liu,[1] Yu Qiao,[2] and Xi Chen[1,a)]
[1]*Columbia Nanomechanics Research Center, Department of Civil Engineering and Engineering Mechanics, Columbia University, New York, New York 10027-6699, USA*
[2]*Department of Structural Engineering, University of California at San Diego, La Jolla, California 92093-0085, USA*

(Received 4 January 2008; accepted 25 January 2008; published online 13 March 2008)

Pressure-driven liquid infiltration into hydrophobic nanoporous solids has important applications for energy absorption. Using water infiltration into a carbon nanotube as a model system, here we show from molecular dynamics simulation that with applied charges, the effective degree of hydrophobicity can be increased, which leads to an improved adjustability of energy absorption efficiency. The attractions exerted by the charges can facilitate initial water infiltration, but they may also stick the molecules and effectively block the pathways of subsequent water entrance. Higher pressure is thus needed to infiltrate water into the tube when external charges (or electrical fields) are applied. © *2008 American Institute of Physics*. [DOI: 10.1063/1.2857474]

Owing to their large specific surface area, carbon nanotubes (CNTs) and nanoporous materials are excellent nanoconduits in nanofluidic devices for molecular transport, with potential applications, including nanopipets,[1] biomolecule separation,[2] molecule detection,[3] and recently, energy absorption and damping.[4,5]

In a nanoporous energy absorption system (NEAS), hydrophobic nanoporous particles are embedded in a nonwetting liquid. When an external pressure is applied, the liquid is forced to infiltrate the nanopores and at a critical (infiltration) pressure, the capillary force can be overcome; that is, the external work is converted to interface energy between the solid and liquid phases, with potential energy absorption density much higher than that of conventional systems.[6] In order to understand the intrinsic infiltration behavior, theoretical and numerical studies are necessary to guide the experiments and design of nanofluidic devices/NEAS.

In essence, the nanofluidic behavior is dominated by interface characteristics, and extensive molecular dynamics (MD) simulations have been carried out for studying the transport behavior of water inside CNTs.[6–8] Since an external electrical field may strongly influence the behavior of dipolar liquids in nanoenvironments and affect the solid-liquid interface tension,[9] it becomes attractive to control nanofluidic behavior using electrical fields.[10,11]

Most previous research focus on the transport behavior of water inside CNTs; however, with respect to the tremendous potential in developing advanced energy absorption systems and volume-memory liquids based on NEASs,[4,10,11] it is important to study the pressure-induced infiltration as well as how this can be affected or controlled by an applied electric field. From a theoretical point of view, it is interesting to explore the variation of infiltration pressure (and, hence, the energy absorption efficiency) when a NEAS is modified by point charges and their underlying molecular mechanisms.

MD simulations are carried out to explore the effect of applied charges on the pressure-driven water infiltration into nanopores. A normally hydrophobic (15,15) CNT [Ref. 8] (inset of Fig. 1), is employed as a model nanopore in a NEAS. The bottom end of the tube is immersed into a reservoir, which is bounded by two rigid planes of atoms in the axial (vertical) direction, and periodical boundary conditions are applied in the transverse directions. Initially, the reservoir ($55\times55\times35$ Å^3) is filled with 3542 water molecules (inset of Fig. 1) such that the normal water density at 1 atm is maintained. We study two embodiments, one without charges and another with charges. In the latter case, 12 point charges are placed at the bottom end of the tube, all of which are fixed at 0.8 Å away from the nanopore boundary in the radial direction, forming a charge ring attached to the nanopore. The same absolute value of $2e$ is assumed for all charges, with the sign altering between neighboring charges so as to keep the designed system electrically neutral. The described modifications of NEASs via charges could be realized by producing functional groups in appropriate positions.[12]

MD simulations are carried out at 300 K by using condensed-phase optimized molecular potentials.[13] By mov-

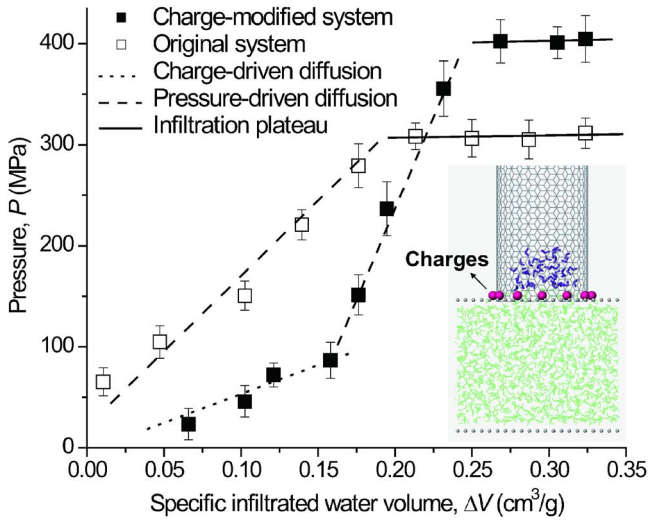

FIG. 1. (Color online) The relationships between the effective reservoir pressure P and SIWV ΔV for tubes without charge and for tubes with charges.

a)Electronic mail: xichen@civil.columbia.edu.

ing the bottom rigid plane (piston) upward, the effective pressure of water in the reservoir is controllable. This pressure can be computed from the change of water density via the state function of water. After each loading increment, the piston is stopped until a new system equilibrium is reached, followed by the statistics of the specific infiltrated water volume (SIWV) (which is the infiltrated water volume divided by the mass of the CNT segment wetted by the end of simulation). At a very slow loading rate, the process is close to being quasistatic. The inset of Fig. 1 is a snapshot of the profile of the water molecules that have infiltrated as the piston is moved up for 2.8 Å from its original position.

The relationships between the SIWV variation ΔV and the *effective* reservoir pressure P are given in Fig. 1. In the absence of charge, the infiltration behavior exhibits two linear stages: (i) At a moderate pressure, water molecules can enter the CNT via surface diffusion because diffusion near the tube wall is associated with lower energy barrier, as revealed by an energy analysis elaborated below. With increased pressure, more water molecules with higher potential energy are capable of entering the CNT, and thus in the first stage, the SIWV varies almost linearly with pressure. (ii) As the critical (infiltration) pressure (about 310 MPa) is reached, the energy of bulk water molecules is sufficiently high to overcome the most significant energy barrier and help bulk water enter the tube with no further external efforts required. Thus, beyond the critical pressure P_{in}, the infiltrated water volume significantly increases and eventually approaches a steady state (spontaneous water entrance). The infiltration pressure decreases with increase in tube diameter (i.e., the increase in the area accessible to water entrance).

The behavior of the charge modified system is different and shows three distinct stages. In the first two stages, the SIWV varies linearly with pressure but with distinct slopes. The first stage is charge-driven diffusion with a fast water entrance rate. The second stage is pressure-driven diffusion but its rate is significantly lower than that in the absence of charge, and the third infiltration stage also has a critical P_{in} that is about 100 MPa higher than that without charge. Since the specific energy absorption density is the area enclosed by the P-ΔV curve in Fig. 1, the charge modified system encompasses higher potential of energy absorption, and thus it is apparently more hydrophobic; the detailed mechanism arises from the attraction between applied charges and polar water molecules, which is analyzed below.

As a bulk water molecule (from the reservoir) enters a nanopore, it needs to lose about two of its hydrogen bonds[8] and interact with the solid atoms of the nanopore. These changes will cause a variation in system potential (positive for hydrophobic nanopores and negative for hydrophilic nanopores), which explicitly determines whether or not the infiltration behavior is energetically favorable. For nanopores that exhibit apparent hydrophobicity, such as CNTs, the water molecules need to overcome the energy barrier via thermal fluctuation and increased potential energy due to the applied pressure. With applied charges, the water molecules are also subjected to electrostatic interactions, whose attraction would greatly lower the energy barrier near charge sites and thereby facilitates water entrance in the first stage, and this term is also responsible for the different infiltration behaviors in the second and third stages.

While the energy associated with the loss of hydrogen bonds is essentially invariant, the interactions with C atoms

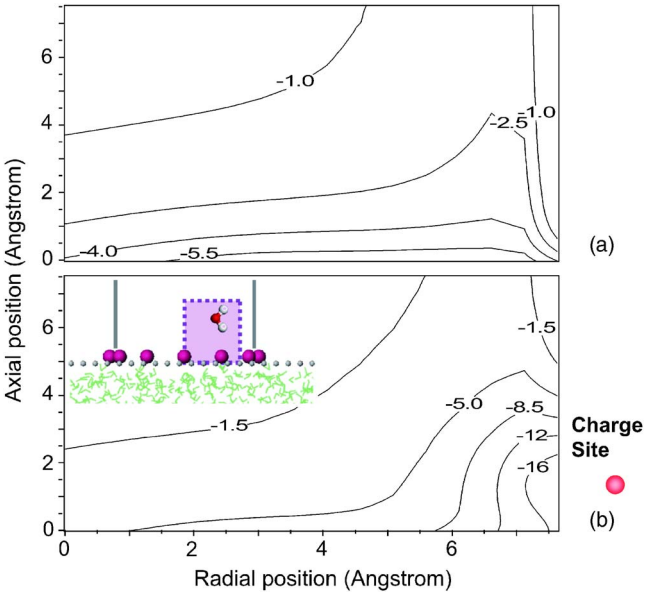

FIG. 2. (Color online) Interaction energy maps of a single water molecule inside the tube: (a) system without charge and (b) charge modified system.

and with charges are dependent on the position of the entry water molecule. Consider a H_2O molecule whose position is varied in an area near the nanopore opening (about 3 Å from the CNT boundary, inside the box in the inset of Fig. 2). For each position, the O atom of the examined water molecule is fixed and the two H atoms are positioned according to optimization of the system potential energy (which also corresponds to the minimized interaction energy, since the potential energy of a single water molecule is negligible and all other energies are unchanged). The resulting interaction energy maps are plotted in Fig. 2.

Figure 2(a) shows different levels of potential energy barriers that need to be overcome so that a single water molecule may reach a certain position; the isolines are analogous to profiles of the infiltrated water front as the potential energy is accumulated. It is readily seen that water molecules prefer to stay close to the CNT wall due to van der Waals interaction, and that would lead to the formation of a shell with concentrated water molecules near the nanopore inner surface, also known as the first solvation shell.[14] Therefore, even at moderate pressures, water molecules can still enter the nanopore via surface diffusion from the first solvation shell toward the interior of the tube. On the other hand, there exists an obvious energy gradient along the tube axis, indicating that the front of the infiltrated water segment needs increasing assistance to proceed toward the interior of the tube. This is the pressure-driven surface diffusion shown in Fig. 1.

By contrast, according to Fig. 2(b), deep potential energy well is found around the attached point charge. In other words, the interaction energy is greatly reduced when a polar water molecule approaches the charge ring, thus significantly promoting the water entrance rate at the beginning (first stage). Meanwhile, the energy well also makes it difficult for attracted water molecules to escape. Therefore, after the initial stage of charge-assisted diffusion, some water molecules appear to be stuck by the point charges and effectively "block" the subsequent entrance of other H_2O molecules. Under this circumstance, the formation of the first solvation shell becomes difficult, and the surface diffusion mechanism

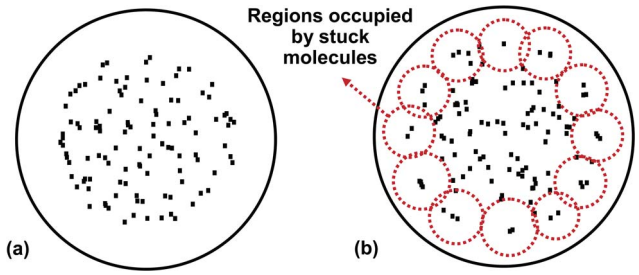

FIG. 3. (Color online) Penetration of water molecules through the entry plane: (a) entry sites of the original NEAS and (b) entry sites of the charge enhanced NEAS.

would not work well, which then requires a much increased pressure to assist more liquid molecules to circumvent the prior "blocking" water molecules and enter the nanopore—this is the pressure-driven diffusion (second stage of the charge modified system), whose diffusion rate is significantly slower than that without charge (Fig. 1).

With continued increase in P, at a critical pressure the liquid can continuously flow into channels without additional assistance, as observed in the last stage in Fig. 1 for both systems. Denote $\Delta\gamma$ as the excessive solid-liquid interfacial tension of the infiltrated liquid segment, whose effective diameter is D; equilibrium dictates the effective infiltration pressure $P_{in}=4\Delta\gamma/D$, which is known as the Laplace–Young equation. From an atomistic point of view, when the infiltrated segment is sufficiently long such that the end boundary effect becomes negligible, the system potential variation associated with the stabilized interaction energy and the loss of hydrogen bonds represent the ultimate energy barrier that bulk water needs to overcome, initiating spontaneous infiltration without additional pressure increase. The energy barrier normalized by the lateral area of occupied nanopore segment is $\Delta\gamma$. Far away from the tube ends, $\Delta\gamma$ is the same for the two systems and, as will be shown below, it is the smaller D that leads to the higher P_{in} in the charge modified NEAS.

To validate the above findings, in particular, the blocking mechanism of the water molecules "attached" to the charges near the tube opening, the trajectory of every water molecule is analyzed to explore where it has penetrated the entry plane of nanopore. The results are shown in Fig. 3; each point represents the entry location of a H_2O molecule on the entry plane, and by the end of the infiltration, every entry molecule would leave one such mark. Due to the electrical static attraction, the area accessible to H_2O is seemingly enlarged after point charges are applied. However, such an apparently larger accessible area does not lead to a lower infiltration pressure (Fig. 1), owing to the existence of the regions occupied by "stuck" molecules. These regions, circled by dash lines in Fig. 3(b) and corresponding to the potential energy wells shown in Fig. 2(b), are centered by about one to three stuck H_2O molecules in each case, effectively blocking the pathways of other molecules. Hence, D, the effective diameter of the water segment entering the tube, is smaller when external charge is present. From Fig. 3, D is estimated to be 3.52 Å for the original NEAS and 2.68 Å for the charge modified NEAS. The product of P_{in} and D is computed as 0.1092 N/m for the original NEAS and 0.1072 N/m for the charge modified NEAS, matching well with Young's equation and thus validating the blocking mechanism.

TABLE I. Water flux through different subregions of the observation plane; comparison of the fluxed across different subregions and of the fluxed in systems without and with charges.

	Inner and outer radii of annular subregions (Angstrom)						
	0–1	1–2	2–3	3–4	4–5	5–6	>6
Modified system	0.08	0.13	0.18	0.16	0.21	0.11	0.13
Original system	0.14	0.19	0.13	0.14	0.13	0.07	0.20

Another evidence of the blocking mechanism is the flux across the entry plane, which is divided into seven annular subregions in Table I, numbered from the center of tube. The water volume passing through each subregion (normalized by the total infiltration volume) depicts the preferred location of water flux entrance. Without charges, water prefers to enter via surface diffusion (region 7, where the first solvation shell is located) during the first stage and via pressure-driven infiltration (regions 1 and 2) during the second stage. For the charge modified system, to circumvent molecules stuck in region 7, the water molecules have entered primarily through regions 3–5.

In summary, we report several mechanisms governing the pressure-driven infiltration of water into a CNT with external charges applied. First, the attractive forces exerted by the charges facilitate water entrance in the beginning. The attraction also forms deep energy wells, which tend to reduce the mobility of the entry water molecules and stick them. Subsequently, the blocking effect imposed by these stuck molecules lowers the area accessible to subsequent water entrance, decreasing the effective radius of the nanopore and leading to a significant increase in effective infiltration pressure. Thus, it is predicted that with applied charges/electrical field, the energy absorption density of a NEAS can be adjusted. Specific arrangement of charges and compositions of polar liquid molecules may be sought so as to make the energy well of charges more prominent and to further enhance the effective degree of hydrophobicity of the system.

The study was supported by the National Science Foundation under Grant No. CMMI-0643726.

[1]M.-H. Hong, K. H. Kim, J. Bae, and W. Jhe, Appl. Phys. Lett. **77**, 2604 (2000).
[2]K. B. Jirage, J. C. Hulteen, and C. R. Martin, Science **278**, 655 (1997).
[3]D. W. Deamer and M. Akeson, Trends Biotechnol. **18**, 147 (2000).
[4]A. Han and Y. Qiao, J. Mater. Res. **22**, 644 (2007).
[5]X. Chen, F. B. Surani, X. Kong, V. K. Punyamurtula, and Y. Qiao, Appl. Phys. Lett. **89**, 241918 (2006).
[6]Y. Qiao, G. X. Cao, and X. Chen, J. Am. Chem. Soc. **129**, 2355 (2007).
[7]A. Striolo, Nano Lett. **6**, 633 (2006).
[8]G. Hummer, J. C. Rasaiah, and J. P. Noworyta, Nature (London) **414**, 188 (2001).
[9]S. Vaitheeswaran, J. C. Rasaiah, and G. Hummer, J. Chem. Phys. **121**, 7955 (2004).
[10]X. Kong and Y. Qiao, J. Appl. Phys. **99**, 064313 (2006).
[11]A. Han and Y. Qiao, Appl. Phys. Lett. **91**, 173123 (2007).
[12]N. Chopra, M. Majumder, and B. J. Hinds, Adv. Funct. Mater. **15**, 858 (2005).
[13]H. Sun, J. Phys. Chem. B **102**, 7338 (1998).
[14]J. M. Heuft and E. J. Meijer, J. Chem. Phys. **119**, 11788 (2003).